Scientific Research Publishing

Atmospheric and Climate Sciences, 2025, 15(4), 788-815
https://www.scirp.org/journal/acs
ISSN Online: 2160-0422
ISSN Print: 2160-0414

Long-Term Merra-2 Characterization of Black Carbon's Surface Mass Concentrations and Its Impact to Climate Change over East Africa

Jacob W. Kutoto[1*], John W. Makokha[1], Tom Ekisa[2], Geoffrey W. Khamala[1]

[1]Department of Science, Technology and Engineering, Kibabii University, Bungoma, Kenya
[2]Department of Biological and Environmental Science, Kibabii University, Bungoma, Kenya
Email: *makokhajw@kibu.ac.ke

How to cite this paper: Kutoto, J.W., Makokha, J.W., Ekisa, T. and Khamala, G.W. (2025) Long-Term Merra-2 Characterization of Black Carbon's Surface Mass Concentrations and Its Impact to Climate Change over East Africa. *Atmospheric and Climate Sciences*, **15**, 788-815.
https://doi.org/10.4236/acs.2025.154040

Received: July 3, 2025
Accepted: September 27, 2025
Published: September 30, 2025

Abstract

Black carbon (BC), which is one of the short-lived climate forcers, largely influences the local modulation of the climate, particularly in regions that are sensitive such as East Africa. However, the long-term trends and meteorological impacts of BC in this region remain not very well investigated, especially considering the context of altered anthropogenic and natural emission sources. This study bridges this gap through a comprehensive spatio-temporal examination of BC surface mass concentration for East Africa from 1980 to 2023 using data from the Modern-Era Retrospective Analysis for Research and Applications, Version 2 (MERRA-2). It has also established statistical correlation between BC concentrations and the selected meteorological parameters, *i.e.*, surface air temperature, specific humidity, surface wind speed, and total surface precipitation. Time-series analysis, spatial visualization, and Pearson correlation were applied to analyze the MERRA-2 datasets. Results showed pronounced intra- and inter-annual variability in BC distribution with high concentrations ($>8 \times 10^{-12}$ kg/m^3) mostly over western Uganda and northwestern Kenya and Tanzania during boreal winter. Such space hotspots were linked to both local sources (biomass burning, automobile pollution) and long-range atmospheric transport from Asian and Middle Eastern industrial regions. The effect of natural sources such as West African bushfires and Saharan dust storms, was also reflected by transboundary dispersion patterns due to wind systems in operation. Correlation analysis found that surface wind speed showed a statistically significant negative correlation with BC concentrations during all seasons, particularly March-May ($r = -0.57$, $R^2 = 0.31$) and June-August ($r = -0.51$, $R^2 = 0.24$), indicating high winds favour BC dispersion. Specific humidity in addition to precipitation was moderately positively correlated with BC, particularly during the September-November season (r =

0.47, $R^2 = 0.20$), showing complex interactions between atmospheric moisture and aerosol lifecycles. Surface air temperature was most strongly seasonally correlated with BC during the short rains ($r = 0.55$, $R^2 = 0.29$), showing the two-way effect of BC on atmospheric warming and radiative forcing. In short, the investigation indicates that BC concentrations over East Africa exhibit distinct spatial and temporal patterns driven by both human and natural processes. The statistically significant correlations with meteorological parameters prove the modulating role of BC in regional climate processes. Policymakers must prioritize emission control actions targeted at biomass burning and urban pollution, and scientists must keep investigating high-resolution BC-climate interactions using integrated ground and satellite observations to advance climate impact assessment in East Africa.

Keywords

Black Carbon, MERRA-2, East Africa

1. Introduction

Black carbon (BC) is an important component of fine particulate matter ($PM_{2.5}$), consisting of carbonaceous particles produced by the incomplete combustion of fossil fuels, biomass, and biofuels [1]. As a potent short-lived climate forcer (SLCF), BC plays a significant role in climate change with its strong ability to absorb solar radiation and directly heat the atmosphere [2] [3]. The radiative characteristic of BC not only heats the atmosphere but also changes cloud microphysics, surface albedo, regional precipitation patterns, and thermodynamic stability of the atmosphere [4]. Due to these multiple pathways of influence, BC is currently deemed the second most important anthropogenic force of global warming after carbon dioxide [5].

Urbanization, population growth, industrialization, and increasing reliance on biomass fuels in East Africa have completely altered local emission profiles. Sources such as vehicle emissions, household combustion of biomass, and agricultural burning have created high concentrations of black carbon across the region. Additionally, East Africa is affected by natural and trans-boundary sources, including long-range aerosol transport from West African biomass burning and Saharan dust incursions that further increase complexity in the regional BC budget. In spite of its increasing importance for both regional air quality and climate systems, East Africa is underrepresented in long-term BC monitoring efforts due to sparse ground-based observations, high operational costs, and limited spatial coverage [6]. Thus, the region is faced with the challenge of quantifying BC trends accurately and assessing their environmental and health impacts.

To address this critical knowledge gap, this study employs high-resolution reanalysis data from the NASA Modern-Era Retrospective Analysis for Research and Applications, Version 2 (MERRA-2). MERRA-2 blends observational data with

advanced atmospheric models to generate spatially coherent and temporally continuous datasets, which are a reliable alternative to scattered *in-situ* measurements, especially in data-scarce regions [7]. This research uses MERRA-2 data to analyze black carbon surface mass concentrations over East Africa, namely Kenya, Uganda, and Tanzania from 1980 to 2023.

There are three main objectives of the research: 1) to study long-term annual trends in BC concentrations, 2) to investigate seasonal spatiotemporal patterns, and 3) to estimate statistical relationships between BC and the main meteorological parameters, surface air temperature, specific humidity, surface wind speed, and total surface precipitation. These meteorological variables are both influenced by and influential to BC concentrations, regulating its transport, lifetime, and removal processes through complex feedback mechanisms.

Initial results indicate pronounced intra- and inter-annual variability of BC across the region, with hotspots of spatial concentration over western Uganda, northwestern Kenya, and northern Tanzania, particularly during the boreal winter months. The peaks are sustained by a mix of local emissions and long-range transport from industrialized regions such as South Asia and the Middle East. Correlation analysis reveals statistically significant relationships of BC with meteorological parameters a strongest negative correlation with surface wind speed (indicative of pollutant dispersion) and positive correlations with humidity and temperature, indicating aerosol-cloud-climate interactions.

The study is significant as it provides the first long-term, region wide assessment of BC variability in East Africa derived from MERRA-2 reanalysis data. It contributes significant insight into the role played by black carbon in regional climate processes and provides a scientific foundation for policy development and climate adaptation strategies. The use of reanalysis datasets demonstrates a feasible approach to overcome observational limitations in the developing world for the benefit of both environmental governance and public health planning. Focused controls can bring almost immediate rewards due to black carbon's comparatively short atmospheric lifespan, and East Africa is therefore a significant focus region for intensified research and policy attention.

2. Study Area, Data and Methods

2.1. Study Area

East Africa lies between latitudes (12˚S, 5˚N) and between longitudes (28˚E, 42˚E) within the Eastern Sub-Saharan region of Africa and has a total land-mass area of 1,769,285 km^2. The study was carried out in this region, which comprises Kenya, Uganda and Tanzania as shown in **Figure 1**. East Africa borders Mozambique and Zambia to the south, Burundi and Rwanda to the west, Southern Sudan and Ethiopia to the north, and Somalia and the Indian Ocean to the East. The study domain has a landscape glaciated mountains with inactive volcanoes and permanent snow cover, plateaus and the coastal plain, ranging from sea level to the two tallest peaks of 5895 M (Mt. Kilimanaro) and 3825 M (Mt. Kenya) [8]. It also includes

the world's second-largest fresh water lake by surface area; Lake Victoria which borders Uganda, Tanzania, and Kenya.

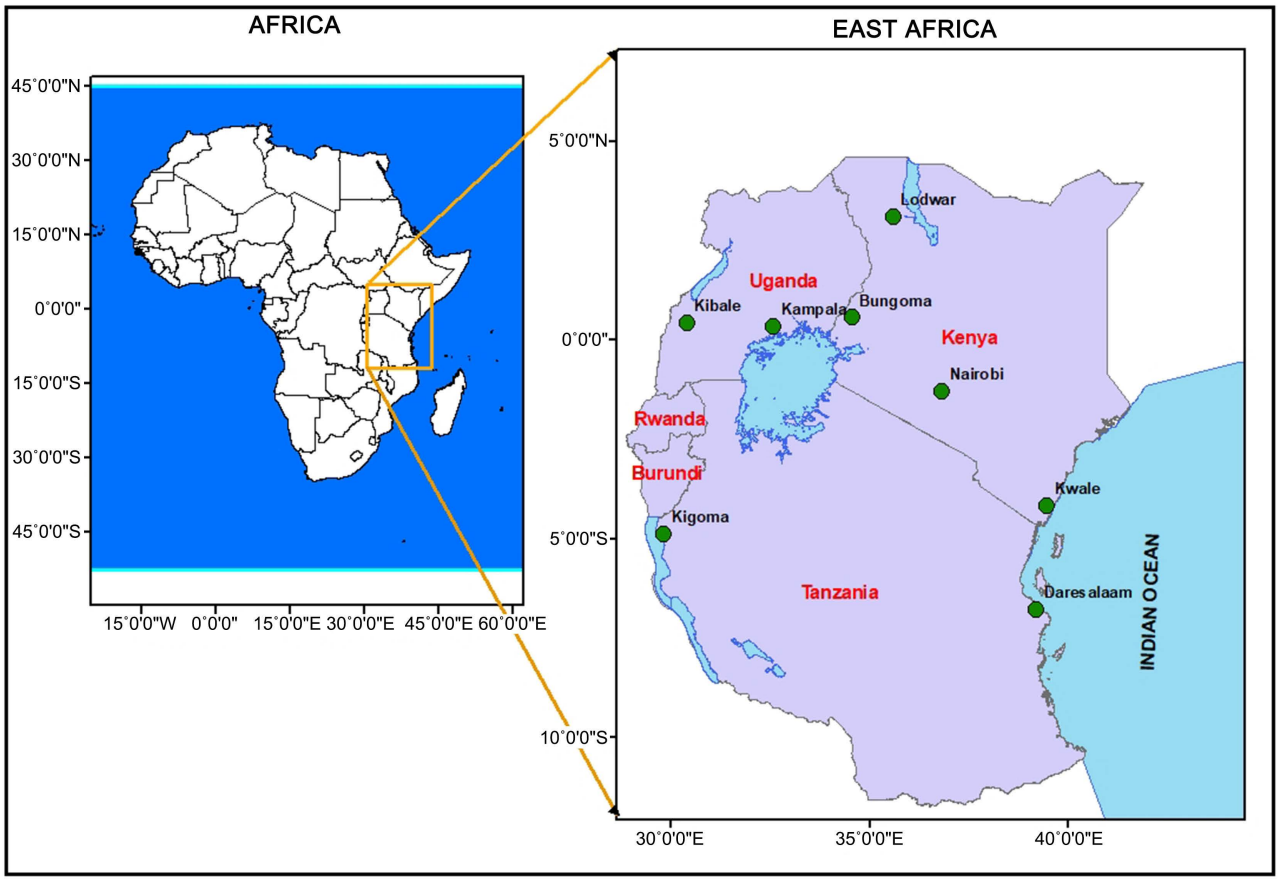

Figure 1. Map of the study area over the African continent (shown in the inset) comprising of Kenya, Uganda and Tanzania. The areas shaded blue represent water bodies; blue labelling shows major lakes in the study domain.

2.2. Local Meteorology

The local meteorology of East Africa is characterized by a diverse range of climatic conditions due to its geographical location and topography. The East Africa has pronounced dry and wet seasons. The dry season, characterized by clear skies and stable atmospheric conditions, can lead to BC accumulation due to limited vertical mixing. In contrast, the wet season with increased rainfall and convective activity can affect aerosol loading and the vertical distribution of BC. The diverse topography of East Africa, including mountains, plateaus, valleys and other physical features that are known to profoundly modify aerosol characteristics in the immediate atmosphere influences local meteorological conditions. Changes in land cover, such as deforestation or urbanization, can impact the regional meteorology and modify the dispersion and deposition of BC particles. The East Africa experiences distinct weather patterns influenced by various factors, such as the Intertropical Convergence Zone (ITCZ), the East African Monsoon, and the El Niño-Southern Oscillation (ENSO). These patterns affect the transport, dispersion, and

deposition of BC aerosols in the region [9].

Surface air temperatures over EA are averagely ranging between 294 K (21˚C) and 298 K (25˚C) with the lowest mean values observed in the months of June to August during the local dry season and highest in the months of December to February (**Figure 2(a)**).

In **Figure 2(b)**, surface specific humidity exhibits notable seasonal variability, ranging from approximately 0.0105 to 0.0145 kg/kg. The highest specific humidity values are observed during the principal wet seasons, namely March-April-May (MAM) and October-November-December (OND). These peaks are primarily associated with the region's bimodal rainfall regime, which is driven by the north-south migration of the Inter-Tropical Convergence Zone (ITCZ) [10].

During these periods, increased convective activity and moisture convergence contribute to enhanced atmospheric moisture content, reflected in the elevated specific humidity levels.

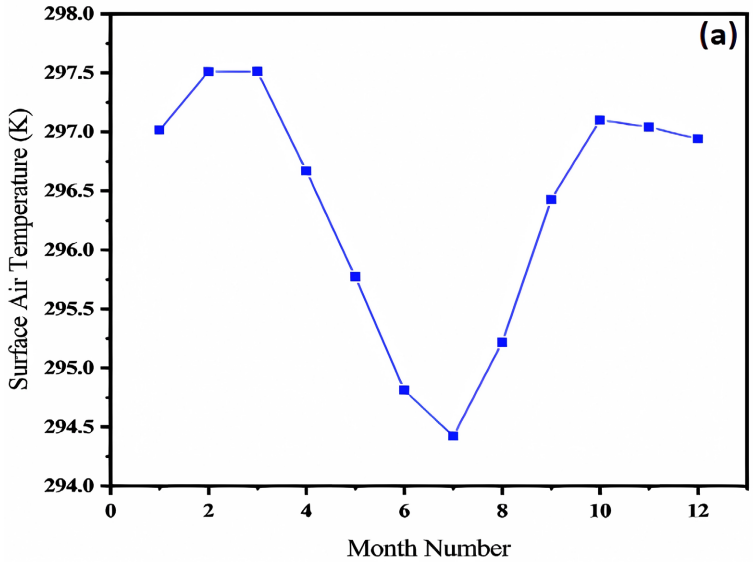

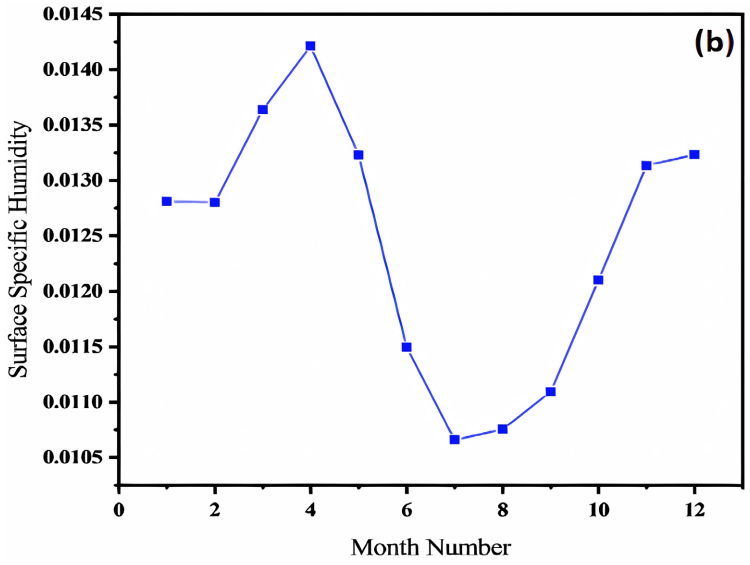

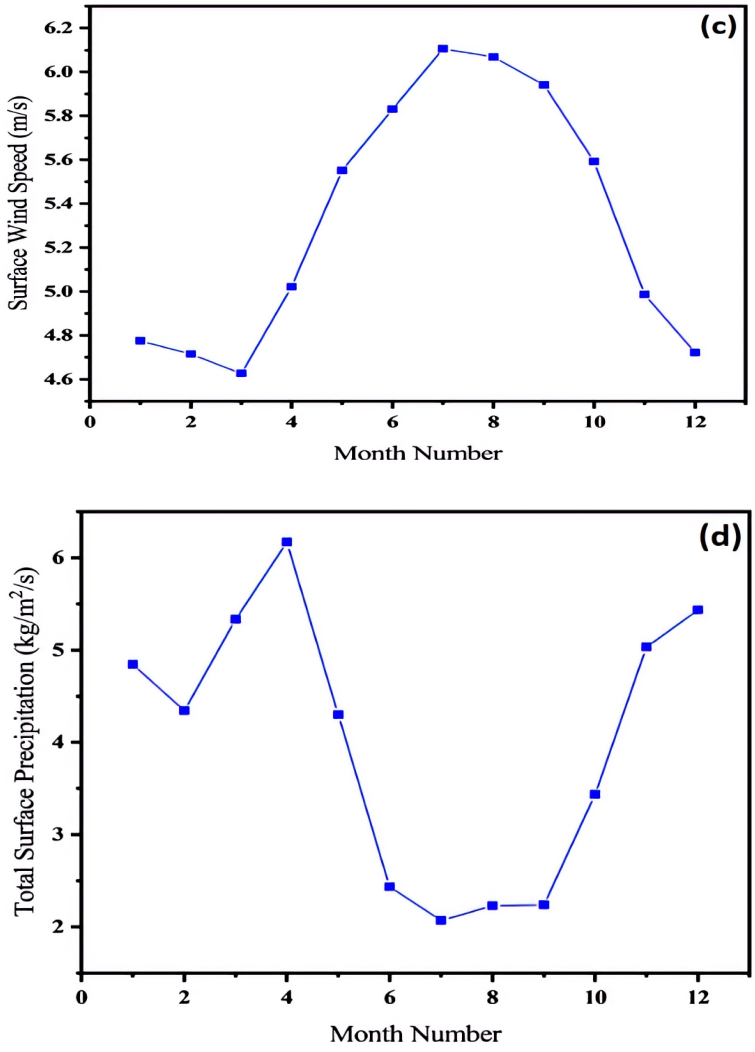

Figure 2. The time series variations of (a) Surface Air Temperature (K), (b) Surface Specific Humidity, (c) Surface Wind Speed ($m \cdot s^{-1}$), and (d) Total Surface Precipitation ($Kg \cdot m^{-2} \cdot s^{-1}$) over East Africa.

Conversely, lower specific humidity values are recorded during the dry seasons—June-July-August (JJA) and January-February (JF). These periods coincide with the ITCZ being positioned away from the region, resulting in subsidence-dominated conditions and reduced moisture availability. Additionally, during JJA, the influence of the Somali Jet and the associated low-level easterlies often advent drier air from the Indian Ocean interior [11], further suppressing humidity levels.

The prevailing winds in East Africa are influenced by the northeast and southeast trade winds, as well as local topography. These wind patterns and atmospheric circulation are vital for the long-range transport of BC particles from both local and distant sources. Surface wind speed showed its maximum value (6.1 m/s) in July minimum mean value in March (4.6 m/s) (**Figure 2(c)**).

The annual total surface precipitation cycle over EA (**Figure 2(d)**) exhibits a

bimodal distribution. The first season, characterized by long rains, which is basically agricultural rains occurs during the March-April-May (MAM). The second season, locally known as "short rains" occurs in October-November-December (**Figure 2(d)**). The local wet seasons are generally characterized with increased BC aerosol surface mass concentration due to large wet deposition and aerosol scavenging from the atmosphere. Another important meteorological phenomenon in East Africa is the Indian Ocean Dipole (IOD). The IOD is a climate pattern characterized by the December short rainy season. Positive IOD events are associated with below-average rainfall in East Africa, while negative IOD events are associated with above-average rainfall [12].

2.3. Data

The Modern-Era Retrospective analysis for Research and Applications, version 2 (MERRA-2), is a state-of-the-art global atmospheric reanalysis dataset developed of NASA's Global Modeling and Assimilation Office (GMAO) in 2009 [7]. MERRA-2 generates a regularly gridded, homogeneous global atmosphere that includes various aspects of the climate system, including aerosols. The model is based on the version of the Goddard Earth Observing System, Version 5 (GEOS-5) atmospheric data from 1980 to 2023 at a spatial resolution of 0.5˚ latitude by 0.625˚ longitude with 72 layers and spanning the satellite era from 1980 to date [13]-[15]. MERRA-2 uses the interactive Goddard chemistry, aerosol, radiation and transport (GOCART) model [16] [17] to simulate the sources, sinks, and chemistry of five externally mixed aerosol species: black carbon, sea salt, mineral dust, organic carbon and sulfate. It provides a comprehensive and consistent record of the Earth's climate system, using a combination of satellite observations, ground-based measurements, and numerical models. MERRA-2 incorporates data from a wide range of sources, including weather stations, satellites, and other observational platforms, to produce a high-resolution, global dataset of atmospheric and surface conditions. MERRA-2 is unique among other models in that it assimilates satellite-made observations of aerosols and represents their interactions with other physical processes [18]. This dataset is used to create a detailed representation of the Earth's climate system, including information on temperature, humidity, wind patterns, and atmospheric composition. Advancing on the success of the atmospheric analysis conducted on GEOS, the current improvements in the MERRA-2 model intend at producing a major Earth System Reanalysis of the atmosphere, land, ocean and ice at a latitude-longitude grid [15]. In the present study, MERRA-2 M2TMNXAER_5_12_4_BCSMASS monthly area-averaged map data for Black Carbon Surface Mass Concentration at a spatial resolution of 0.5˚ × 0.625˚ from 1980 to 2023 were retrieved for monthly and seasonal trends analysis and MERRA-2 M2TMNXAER_5_12_4_BCSMASS monthly time-averaged data for Black Car-bon Surface Mass Concentration, MERRA-2 M2TMNXFLX_5_12_4_TLML monthly time-averaged data for surface air temperature, MERRA-2 M2IMNXLFO_5_12_QLML monthly time-averaged data for Surface Specific Humidity, MERRA-2 M2TMNXFLX_5_12_4_PRECTOT

monthly time averaged data for Total Surface Precipitation and MERRA-2 M2TMNXFLX_5_12_4_SPEED monthly time-averaged data for surface Wind Speed at a spatial resolution of 0.5˚ × 0.625˚ from 1980 to 2023 were retrieved for correlation analysis. These data products were sourced from http://Giovanni.gsfc.nasa.gov/Giovanni/.

2.4. Methodology

2.4.1. Linear Regression Analysis

Raw data files were downloaded from NASA's online archives, encompassing monthly records from 1980 to 2023. These individual files were merged into a unified dataset using Climate Data Operators (CDO) software. This consolidation ensured temporal continuity necessary for robust trend analysis.

Similar to established methodologies in climate science [19] [20], monthly and seasonal trends in black carbon surface mass concentration were assessed using the grid-wise linear trends approach. This methodological choice was justified by its capability to discern temporal variations in long-term datasets effectively.

The monthly black carbon surface mass concentration (BCSMC) data (Y_t) were modelled using a simple linear trend equation:

$$Y_t = aX_t + b + N_t, t = 1, \cdots, T \tag{1}$$

where (Y_t) represents the black carbon surface mass concentration at time (t), (X_t) denotes the independent variable indicating the time series ($X_t = \frac{t}{44}$, where t is specific month in time series), 1) signifies the assessed trend in black carbon surface mass concentration, 2) represents the offset (y-intercept) indicating the initial black carbon surface mass concentration value, (N_t) accounts for noise in the time series.

The uncertainty (δ) associated with the estimated trend (ω) was evaluated using

$$\delta = \frac{\sigma_N}{n^{3/2}} \sqrt{\frac{1+\Phi}{1-\Phi}} \tag{2}$$

where (σ_N) is the standard deviation of the noise (N_t), (n) is the number of observations, and (Φ) is the correlation coefficient of the noise series.

Significance of the trends was determined using the criteria outlined by [19], with trends considered significant at a 95% confidence level if $\left|\frac{\omega}{\delta}\right| \geq 2$, and at a 90% confidence level if $1.5 \leq \left|\frac{\omega}{\delta}\right| < 2$, Data preprocessing, trend estimation, and uncertainty assessment were performed using MATLAB. Spatial representation of trends across monthly and seasonal intervals was visualized using GrADS (Grid Analysis and Display System) software, facilitating comprehensive spatial analysis and interpretation.

2.4.2. Correlation Analysis

In this study, Origin software was used to analyze the correlation between black carbon surface mass concentration and meteorological parameters. The Pearson

correlation coefficient was calculated using the Correlation Equation below;

$$r = \frac{\sum\left[\left[x_i - \bar{x}\right]\left[y_i - \bar{y}\right]\right]}{\sqrt{\left[\left[\sum\left(x_i - \bar{x}\right)^2\right] x \left[\sum\left(y_i - \bar{y}\right)^2\right]\right]}} \quad (3)$$

where:

x_i and y_i represent the individual values of the two variables being correlated (black carbon surface mass concentration and the selected meteorological parameter).

$\bar{x}$ and $\bar{y}$ represent the means of the respective variables, which quantitatively assessed the linear relationship between the two variables. This method of correlation analysis has been widely used in pipeline risk factors research for identifying and quantifying the impact of key factors such as whether connector, pipe joint length and geological hazards to the detection of non-destructive defects [21]. A scatter plot was created to visually display the data, and a linear regression line was fitted to further examine the relationship. This graphical approach is commonly employed to visualize trends and identify potential linear relationships [22] [23]. The correlation coefficient and the regression line provided insights into the strength and direction of the relationship, with the correlation coefficient value being displayed directly on the plot for easy reference. This analysis allowed for a comprehensive understanding of how black carbon surface mass concentration relates to the selected meteorological parameter, similar to the approach used by [24] to study the estimating infectiousness throughout SARS-CoV-2 infection course

3. Results and Discussion

3.1. Annual Spatial Trends of BC Surface Mass Concentration over East Africa

Figure 3 presents spatial patterns in annual trends of black carbon surface mass concentration and their statistical significance over East Africa from 1980 to 2023. The trends are estimated in terms of increase/decrease and indicated by positive/negative values.

Generally, East Africa exhibits varying BC mass concentration annual trends, with predominantly low, moderate and high positive trends indicating an increase in BC aerosol load. These positive trends could be attributed to the following reasons, 1) industrialization leading to increased anthropogenic aerosol emissions including BC [25] [26], 2) population growth resulting to increased anthropogenic activities [27], 3) climate change occasioned by meteorological parameters such as temperature inversions accompanied by reduced precipitation and wind speed [28] which are favorable conditions for increased aerosol emissions.

The enhanced BC aerosol loading over East Africa could also be attributed to the fact that the study domain is aerosol receptor [29] due to its location between two main aerosol sources. Anthropogenic activities in central Africa where biomass burning activities results in significant amount of BC particles transported

to the northern part of East Africa by the westerlies [30] and natural dust emissions including BC particles from arid and semi-arid lands of north and eastern part of East Africa; alongside those transported from the Saharan and Arabian desert by north easterlies during certain times of the year [31].

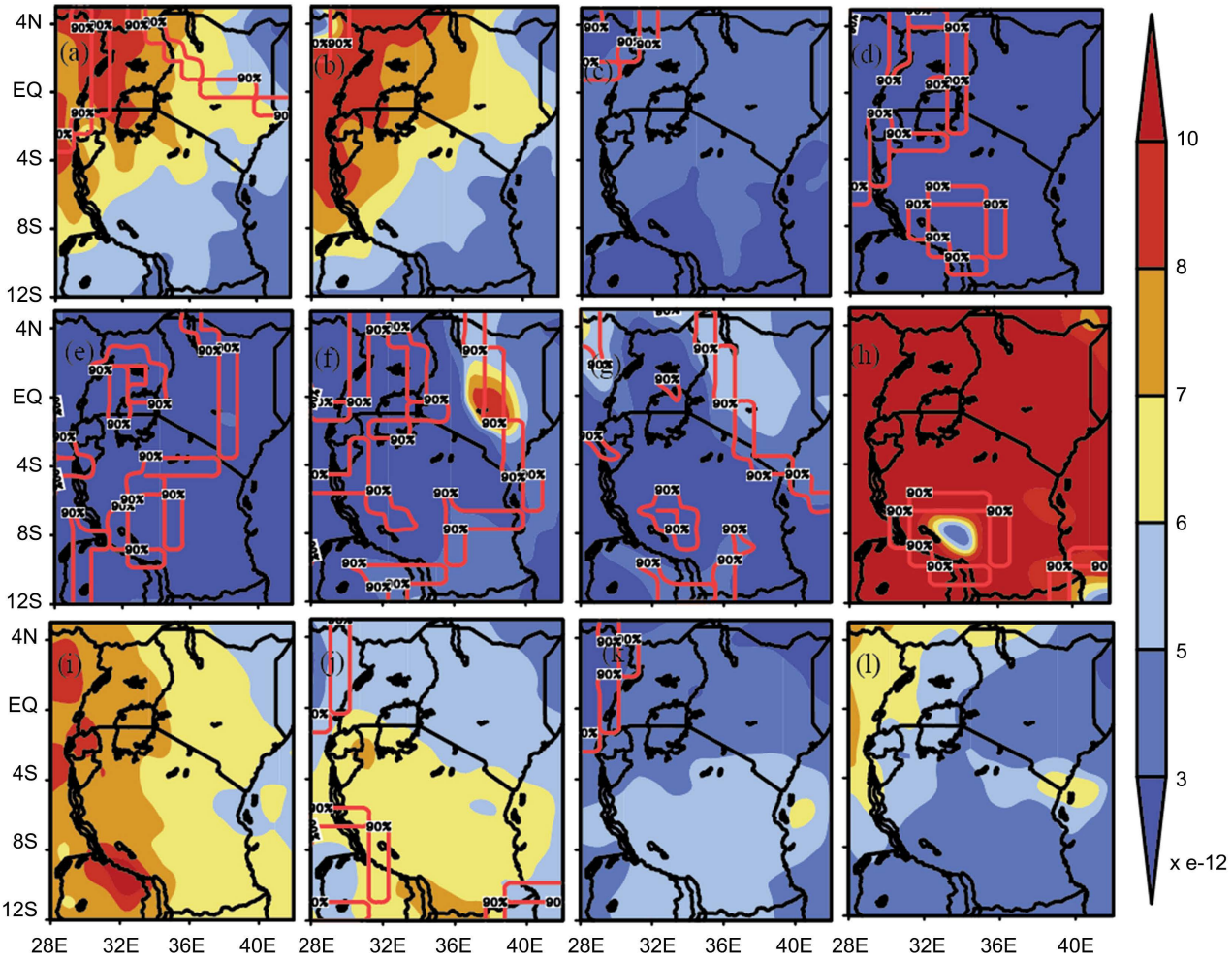

Figure 3. Annual spatial variation of BC Surface Mass Concentration over East Africa using MERRA-2 Model data during 1980-2023 period.

The BC mass concentration trends ranged between 3×10^{-12} kg/m^3 to 10×10^{-12} kg/m^3 with lower values $< 5 \times 10^{-12}$ kg/m^3 dominating most parts of the study domain during the wet months and higher values $> 8 \times 10^{-12}$ kg/m^3 during the dry months.

The highest positive monthly trends between 8×10^{-12} kg/m^3 and 10×10^{-12} kg/m^3 and significant at 90% confidence level over East Africa were noticed during the month of August over the study domain. These trends were attributed to local anthropogenic activities arising from biomass burning and industrial-vehicular emissions [32]. Additionally, the transport of black carbon emissions from industrial areas in Asia and the Middle East by easterly winds, as well as natural sources such as wildfires in West Africa and desert storms from the Sahara Desert carried

by westerly winds, contribute to elevated levels of black carbon in East Africa. Highest trends were also noticed in Western Uganda, northwestern parts of Kenya and Tanzania during the months of January and February. These positive trends could be attributed to anthropogenic activities in central Africa and BC particles from Congo rainforest complex which are transported by the westerlies and locally derived air masses that travel at lower altitudes < 1500 m for a shorter distance spending more time hence contributing to the most observed BC aerosol loading.

In June, Nairobi and its surrounding areas exhibit the strongest positive trends July and significant at 90% confidence level in black carbon concentrations, likely due to increased fossil fuel consumption, biomass and refuse burning, and industrial-vehicular emissions in this urban Centre of East Africa.

Moderate BC monthly positive trends from 5×10^{-12} kg/m^3 to 8×10^{-12} kg/m^3 July and significant at 90% confidence level were observed most parts of Kenya except northeastern in September, all parts of Tanzania in October, northwest Uganda in December, western Kenya in January and central part of Kenya in February. The moderate positive trends could be attributed to a combination of biomass burning activities and dust particles including BC particles that are locally derived and due to long-range transport could enhance BC load. Air masses from DRC and Madagascar island carrying fine-mode smoke plumes and locally produced pollutants travel shorter distances spending more time could contribute to BC loading during these periods. However, wet scavenging due to enhanced rainfall patterns could be the reason for moderate trends [32].

During the wet season months of March to July, lower positive trends in black carbon concentrations ranging from 3×10^{-12} kg/m^3 to 5×10^{-12} kg/m^3 July and significant at 90% confidence level are observed, likely due to suppressed emission of black carbon particles by precipitation and reduced biomass burning activities. The influence of the Congo rainforest complex and its associated rainfall patterns may also play a role in shaping these trends, as they impact the regional climate and atmospheric circulation.

3.2. Seasonal Spatial Variations of Black Carbon Surface Mass Concentration over East Africa

Spatial distribution of seasonal trends in BC surface mass concentrations derived from MERRA-2 Model in the units of kg/m^3. The shadings show the sign and magnitude of trends, while the confidence levels are shown as numerals embedded on contours.

Overall, the results of this study highlight the complex interplay of various factors that influence the seasonal trends of black carbon surface mass concentration over East Africa. The seasonal positive trends over most parts of EA imply an increase in load. As outlined in Section 3.2, the magnitudes and signs of trends and relative changes are influenced by both emission and meteorological factors.

During the January-February dry season (**Figure 4(a)**), the study domain ex-

hibits varying BC mass concentration seasonal trends, with predominantly low, moderate and high positive trends indicating an increase in BC aerosol load.

This spatial variations in trends could be attributed to anthropogenic activities in central Africa where biomass burning activities results in significant amount of BC particles transported to the northeastern part of Uganda by the westerlies [30] and natural dust emissions including BC particles from arid and semi-arid lands of north and eastern part of East Africa; alongside those transported from the Saharan and Arabian desert by north easterlies during this dry season [31] [33]. Highest positive trends of between 8×10^{-12} kg/m^3 and 10×10^{-12} kg/m^3 and significant at 90% confidence level dominated most parts of northeastern Uganda. The high positive trend may be linked to local sources of black carbon emissions such as biomass burning for cooking and heating, as well as dust aerosols (locally-derived and due to long-range transport) [34]. Moderate positive trends of 6×10^{-12} kg/m^3 and 8×10^{-12} kg/m^3 were observed in Eastern parts of Uganda, Western parts of Kenya and Northwestern Tanzania and could be influenced by regional transport of black carbon from neighbouring countries, as well as atmospheric circulation patterns that favour the accumulation of pollutants in these areas. Lower trends of 3×10^{-12} kg/m^3 and 6×10^{-12} kg/m^3 are observed in the southern part of Tanzania, the Northeastern part of Kenya and along the coastal region of the study domain. These trends may reflect fewer sources of black carbon emissions and a greater dispersion of pollutants due to prevailing wind patterns in this region since it is an aerosol receptor [29].

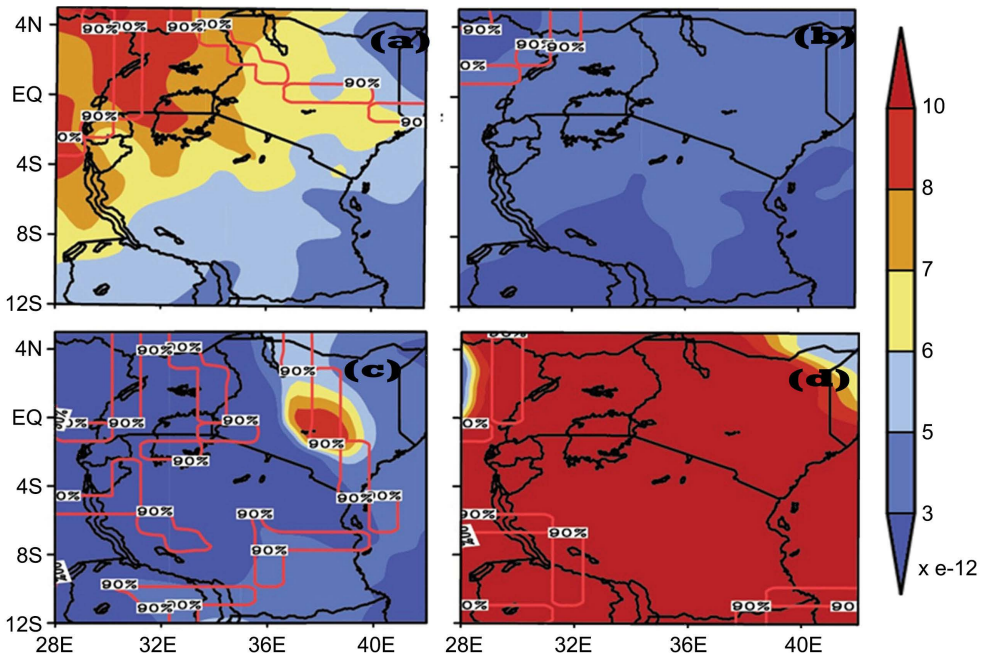

Figure 4. Seasonal spatial variation of BC Surface Mass Concentration using (a) JF, (b) MAM, (c) JJAS and (d) OND seasons over EA during 1980-2023.

In contrast, during the wet season of MAM (**Figure 4(b)**) and SON (**Figure**

4(d)), the trends in black carbon surface mass concentration were generally positive, with low positive trends dominating the study domain. This suggests that black carbon concentrations over the earth's surface tend to increase during the wet season, possibly due to the wet removal of pollutants from the atmosphere and the enhanced deposition of black carbon onto the Earth's surface. The highest trend in black carbon concentration was observed during SON (Figure 4(d)), indicating a peak in pollutant levels during this time of year. This could be attributed to seasonal changes in biomass burning practices, agricultural activities, and meteorological conditions that result in the accumulation of black carbon in the atmosphere.

3.3. Correlation between Trends in Seasonal BC Concentrations and Meteorology

3.3.1. Seasonal Correlation between BC Concentrations and Surface wind Speed

Figure 5 presents the correlations between BC surface mass concentration and surface wind speed for various seasons. The surface wind speed (SWS) is a crucial climate variable that influences the transportation and distribution of aerosols including black carbon from one place to another [35]. This variable is basically influenced by two factors: the friction and pressure gradient. Pressure gradient force is largely generated by temperature difference, with greater temperature disparities leading to stronger winds [36] [37]. The local winds always blow towards low pressure regions hence transporting BC particles from high pressure regions to low pressure regions. On the other hand, friction is caused by obstructions such as tall building and vegetation [38].

The monthly datasets of black carbon surface mass concentration and surface wind speed have been averaged seasonally *i.e.*, local wet (MAM, SON) and local dry (JJA, DJF) seasons during each year. The seasonal correlation between black carbon surface mass concentration and surface wind speed derived from MERRA-2 Model product over East Africa during the study period (1980-2023) are shown in figures above. Across all seasons, the study has shown that surface wind speed had a significant impact on BC concentrations. The study showed that as surface wind speed increased, BC concentrations decreased, indicating that higher wind speeds can help disperse BC pollutants and reduce local concentrations. Moderate negative correlation was observed during December-January-February season (-0.44) in Figure 5(a) and September-October-November season (−0.47) in Figure 5(d) with adjusted R-square values of 0.2060 and 0.2083, respectively. This indicates that approximately 20.60% for (DJF) and 20.88% for (SON) of the variability in black carbon surface mass concentration can be attributed to surface wind speeds. Strong negative correlation was realized during June-July-August season (−0.51) in Figure 5(c) and March-April-May season (−0.44) in Figure 5(b) with adjusted R-square values of 0.24 and 0.31 which indicates that approximately 24% (JJA) and 31% (MAM) of the variability in black carbon surface mass concentration can be attributed to surface wind speeds. The relationship between black car-

bon surface mass concentration and surface wind speed can be explained by the process of atmospheric mixing. Lower wind speeds during the dry seasons can result in reduced atmospheric mixing and dispersion of pollutants, BC particles tend to remain near their source of emission, leading to higher local concentrations. On the other hand, higher wind speeds can help disperse BC particles over larger distances, reducing their concentration at the surface. However, local sources such as traffic emissions and wildfires also contribute to elevated concentrations in certain areas even during period of low wind speed.

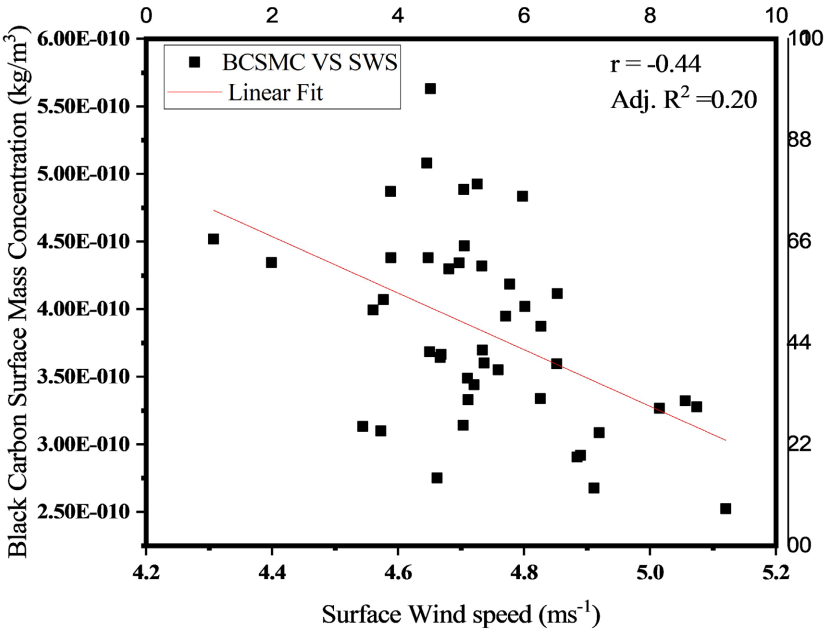

(a)

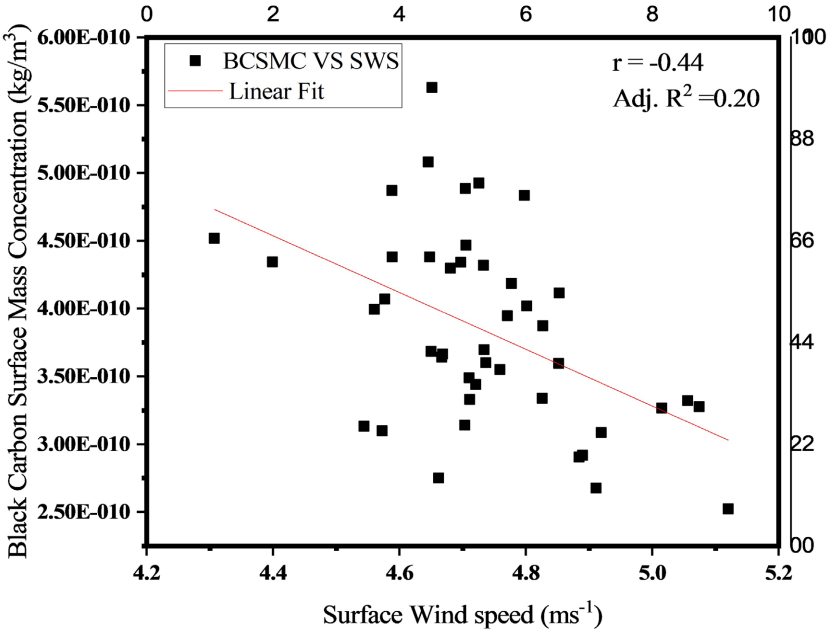

(b)

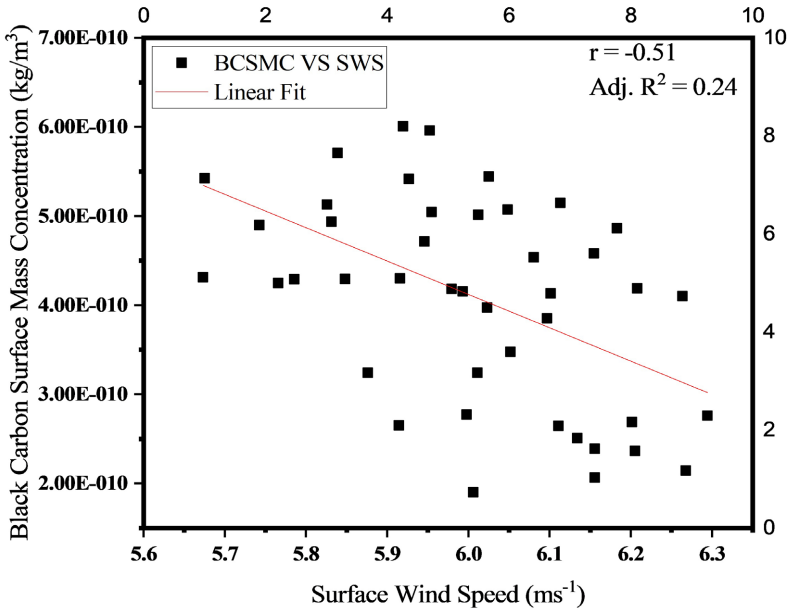

(c)

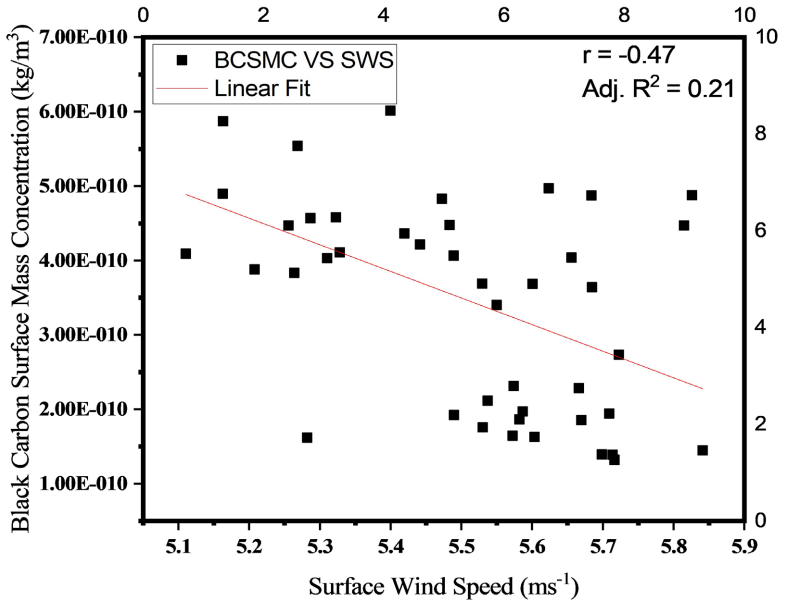

(d)

Figure 5. Seasonal correlation between BC Surface Mass Concentration and Surface Wind Speed averages using (a) DJF, (b) MAM, (c) JJAS and (d) SON seasons over EA during 1980-2023.

Similar results were found by other studies caried out worldwide, a study by [39] in the western United States and a study conducted by [40] in Beijing, China also found a negative correlation between surface wind speed and BC levels.

3.3.2. Seasonal Correlation between BC Surface Mass Concentration and Surface Specific Humidity

The seasonal graphs depicting black carbon (BC) surface mass concentration

against surface specific humidity provide valuable insights into the relationship between these variables in both dry and wet seasons.

During the dry seasons of DJF (**Figure 6(a)**) and JJA (**Figure 6(c)**), the Pearson's correlation coefficients for BC surface mass concentration against surface specific humidity are 0.34. The associated adjusted R-square values of 0.09 indicate that approximately 9% of the variability in BC concentrations can be attributed to surface specific humidity, respectively. These positive but modest correlations suggest a weak relationship between BC surface mass concentration and specific humidity in the dry season. This could be influenced by factors such as regional transport of BC particles, local emissions, and meteorological conditions impacting BC levels [41].

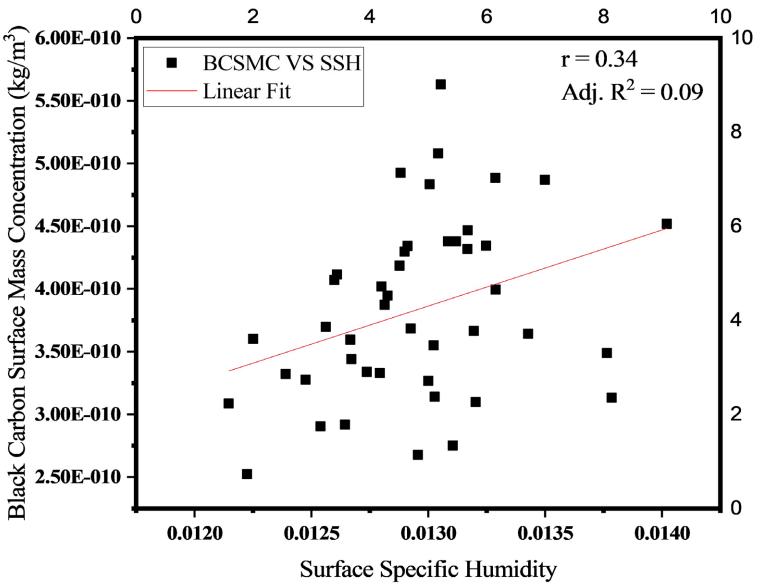

(a)

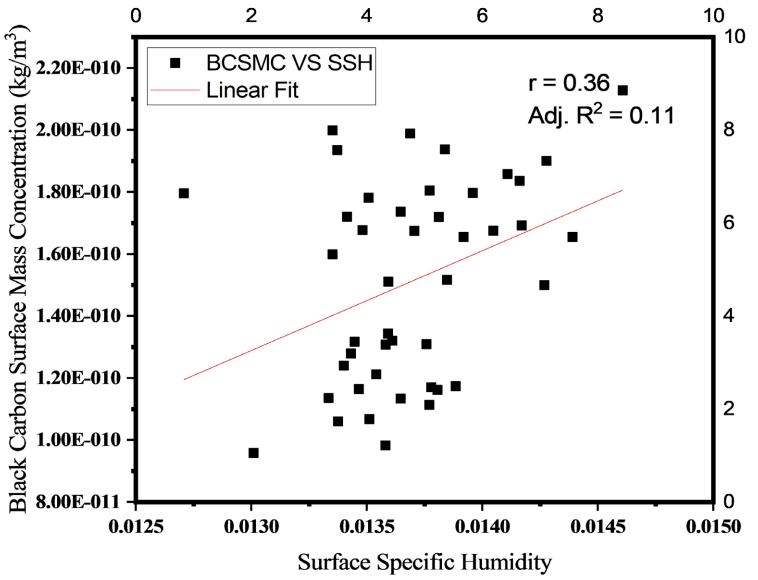

(b)

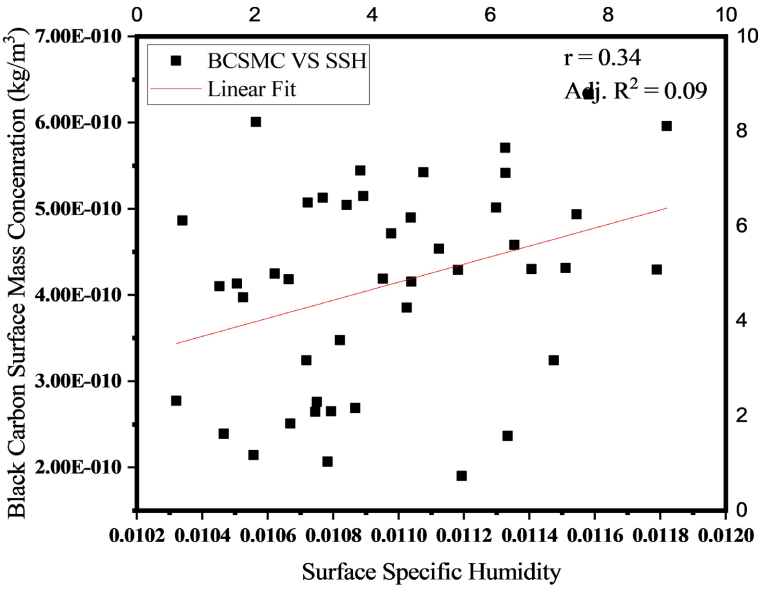

(c)

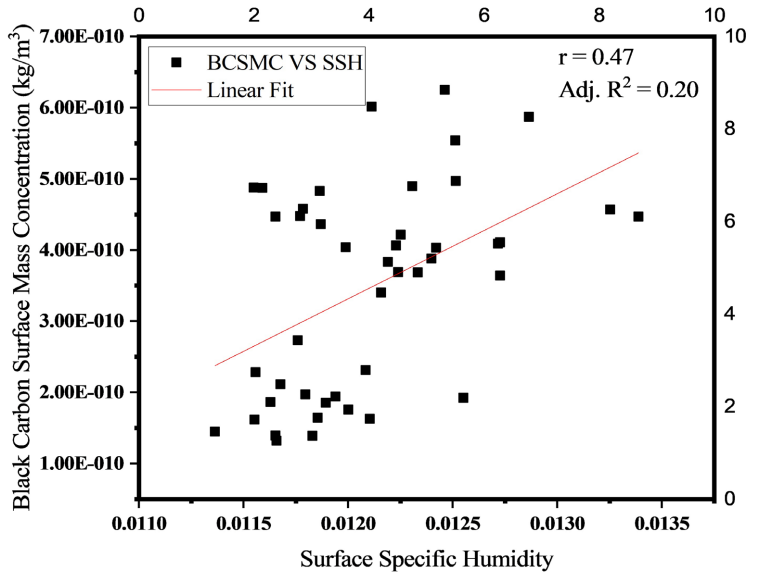

(d)

Figure 6. Seasonal correlation between BC Surface Mass Concentration and Surface Specific Humidity averages using (a) DJF, (b) MAM, (c) JJAS and (d) SON seasons over EA during 1980-2023.

The observed positive correlations between black carbon (BC) surface mass concentration and surface specific humidity during the MAM (March-April-May) (**Figure 6(b)**) and SON (September-October-November) (**Figure 6(d)**) wet seasons, with Pearson correlation coefficients of 0.36 and 0.47, respectively, suggest that increases in humidity are associated with elevated BC levels. The corresponding adjusted R^2 values of 0.11 for MAM and 0.20 for SON indicate that specific humidity accounts for 11% and 20% of the variability in BC concentrations during these seasons. This relationship can be attributed to a combination of meteoro-

logical and emission-related factors. Elevated specific humidity during the wet seasons is often linked to increased atmospheric stability and reduced vertical mixing, which can trap pollutants like BC near the surface. Additionally, although rainfall typically removes aerosols through wet deposition, many humid days during MAM and SON are not rainy, allowing BC to accumulate before precipitation occurs [42]. BC particles may also become internally mixed with hygroscopic species, enabling water uptake that increases their size and atmospheric lifetime [43] Furthermore, road transport emissions may also rise due to poor road conditions during wet periods, leading to inefficient fuel combustion.

3.3.3. Seasonal Correlation between BC Surface Mass Concentration and Total Surface Precipitation

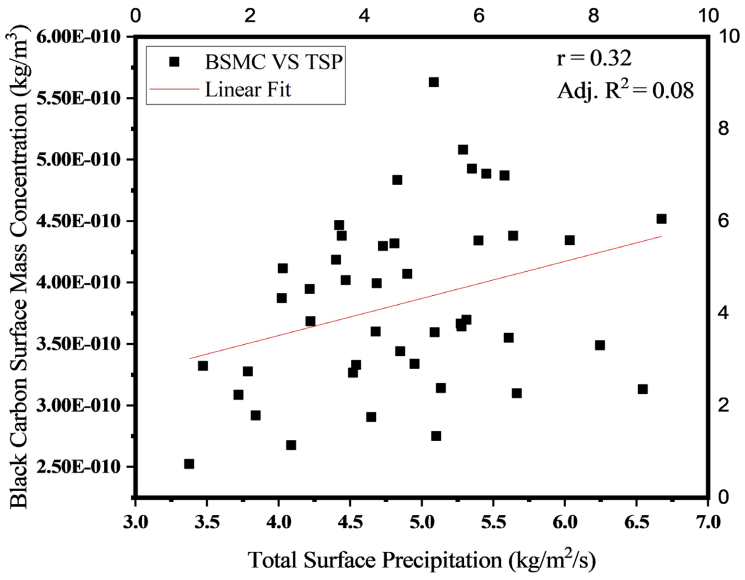

(a)

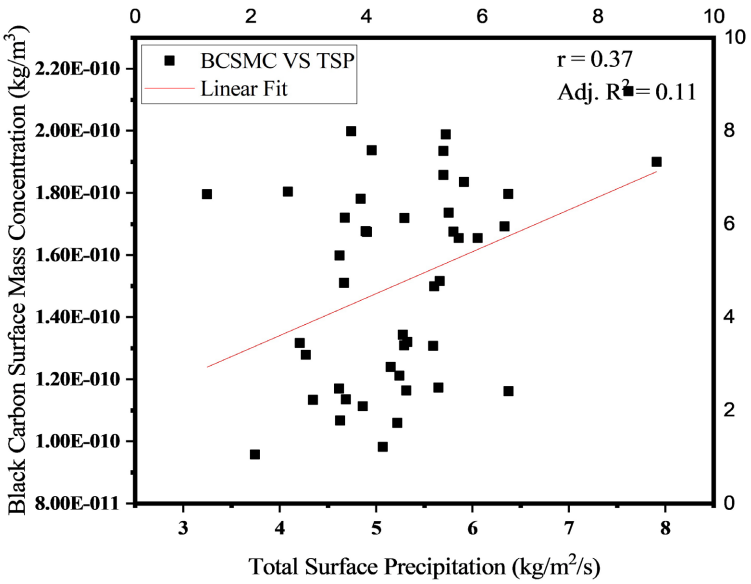

(b)

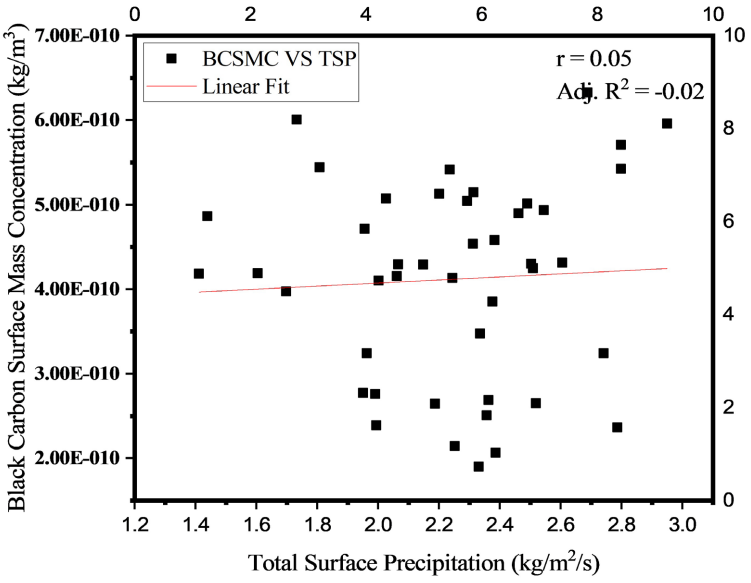

(c)

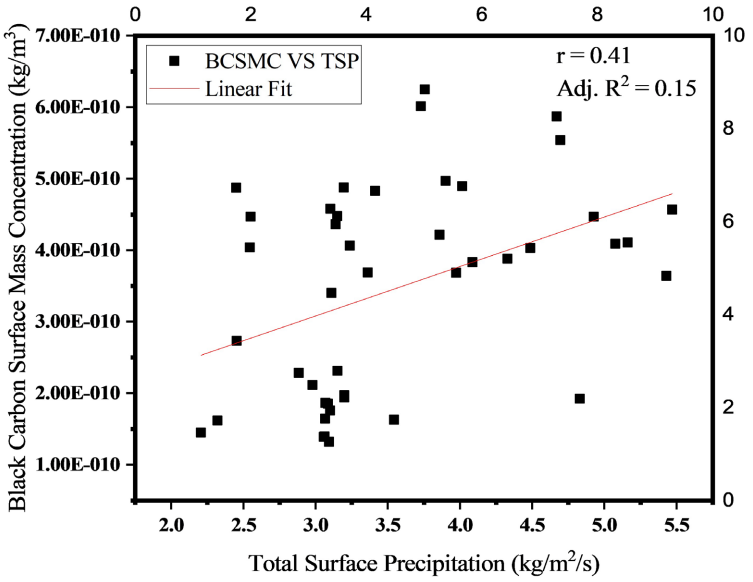

(d)

Figure 7. Seasonal correlation between BC Surface Mass Concentration and Total Surface Precipitation averages using (a) DJF, (b) MAM, (c) JJAS and (d) SON seasons over EA during 1980-2023.

Precipitation has been rated as the main deposition pathway for aerosols including black carbon on the earth's surface. An increase in precipitation translates to a rise in aerosol scavenging from the atmosphere and the prevention of aerosol emissions from the wet surface [44]. In the local dry seasons of DJF (**Figure 7(a)**) and JJA (**Figure 7(c)**), the Pearson's correlation coefficients for BC surface mass concentration against total surface precipitation are 0.32 and 0.06. The associated adjusted R-square values of 0.08 and −0.02 suggest that these models may not adequately explain the variability in BC concentrations based on total surface pre-

cipitation alone. The positive correlation coefficients indicate a weak positive relationship between BC surface mass concentration and total surface precipitation in the dry season. This unexpected positive correlation may be attributed to factors such as long-range transport of BC particles from distant sources, local emissions, and atmospheric mixing processes impacting BC levels [45].

The Pearson's correlation coefficients of 0.37 and 0.41 during the MAM (**Figure 7(b)**) and SON (**Figure 7(d)**) local wet seasons over East Africa indicate a moderate positive correlation between total surface precipitation and black carbon (BC) surface mass concentration. The adjusted R^2 values of 0.11 and 0.15 for MAM and SON indicate that approximately 11% and 15% of the variance in BC concentrations can be attributed to precipitation during the two seasons. This positive though moderate relationship indicates that, in contrast to the typical hypothesis that rain decreases aerosol concentrations due to wet scavenging, there could be other processes simultaneously influencing BC levels along with rain.

In East Africa, rain showers in the wet seasons are typically convective and local, *i.e.*, heavy rain can occur without equally cleansing the atmosphere of pollutants across the region [46]. In addition, instances of increased precipitation can also coincide with high rates of anthropogenic emissions, *i.e.*, cooking, or energy generation through biomass burning, especially in peri-urban and rural areas. Such emissions would have a potential to contribute to increased BC levels even on rainy days. In addition, heavy rain is often preceded by hot, humid, and stagnant atmospheric conditions that can facilitate greater settling of aerosols before they are removed [42]. Transport of BC from neighboring arid regions such as Sahara Desert by shifting wind patterns may also be the cause of high concentrations during wet seasons [34]. Overall, although precipitation influences BC concentration by scavenging, the intensity, timing, and spatial distribution of rain events, and co-emitted sources account for observed positive correlations in East Africa's wet seasons.

3.3.4. Seasonal Correlation between BC Concentrations and Surface Air Temperature

Figure 8 presents the correlations between BC surface mass concentration and surface wind speed for various seasons.

The monthly datasets of black carbon surface mass concentration and surface air temperature were also averaged seasonally *i.e.*, local wet (MAM, SON) and local dry (JJA, DJF) seasons during each year.

Overall, the relationship between black carbon surface mass concentration and surface air temperature is complex and multifaceted, our study found a positive seasonal correlation between black carbon surface mass concentration and surface air temperature, except December-January-February season which has displayed a negative correlation. Strong positive correlation was observed during September-October-November season (0.46) (**Figure 8(d)**) and moderate positive correlation of (0.55) (**Figure 8(c)**) for June-July-August season with adjusted R-square values of 0.19 and 0.29, respectively. This indicates that approximately 19% for (SON) and 29% for (JJA) of the variability in black carbon surface mass concentration can be

attributed to surface air temperature. Weak positive correlation was realized during March-April-May season (0.27) with adjusted R-square value of (0.05) (**Figure 8(b)**) which indicates that only 5% is attributed to surface air temperature.

Several studies done by other researchers have also shown a direct correlation between black carbon surface mass concentration and surface air temperature. For example, a study by [47] found a strong relationship between black carbon emissions and surface temperature in the Arctic region. The study concluded that reducing black carbon emissions could help slow down the rate of warming in the Arctic and mitigate the impacts of climate change. Similarly, [48] demonstrated that black carbon emissions from biomass burning contribute to warming in the Amazon rainforest, leading to changes in rainfall patterns and ecosystem dynamics.

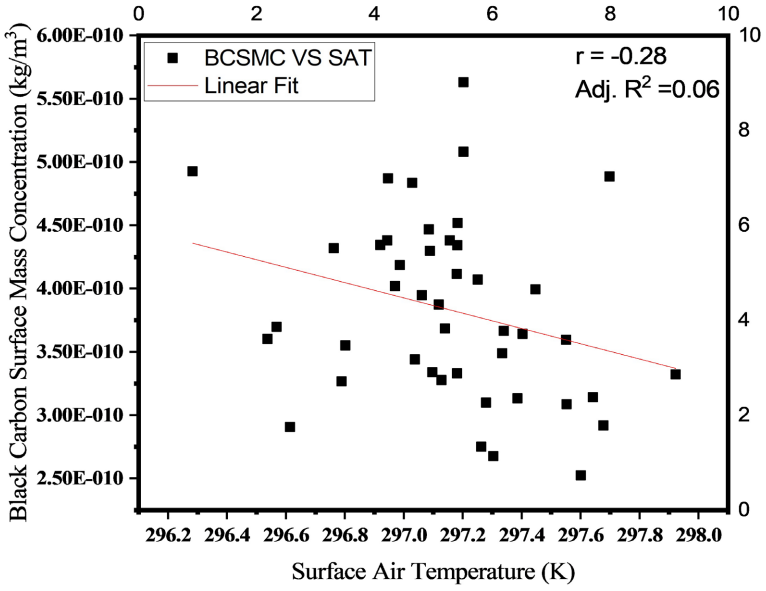

(a)

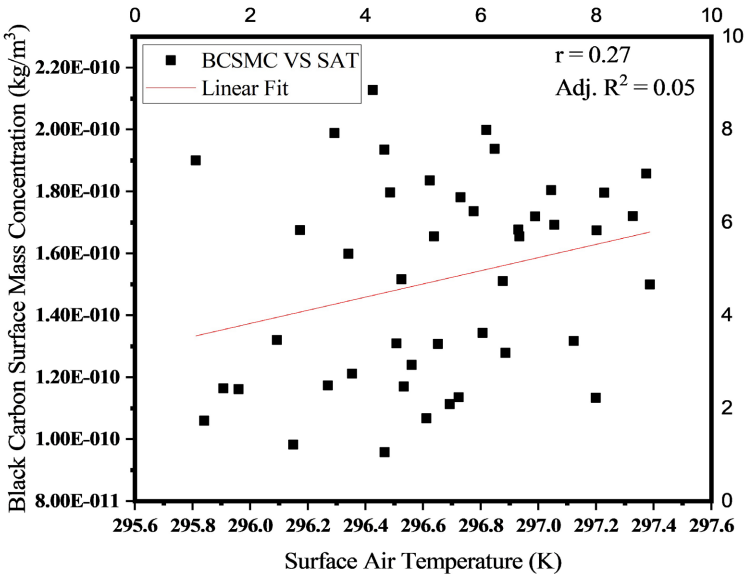

(b)

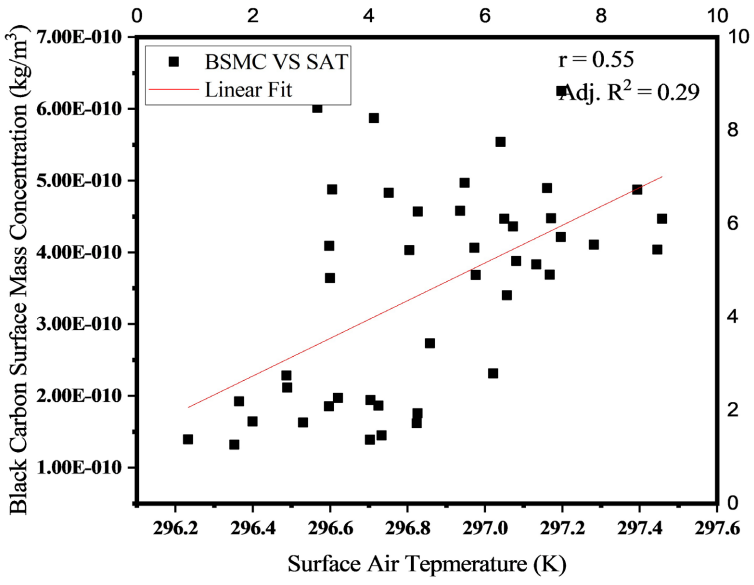

(c)

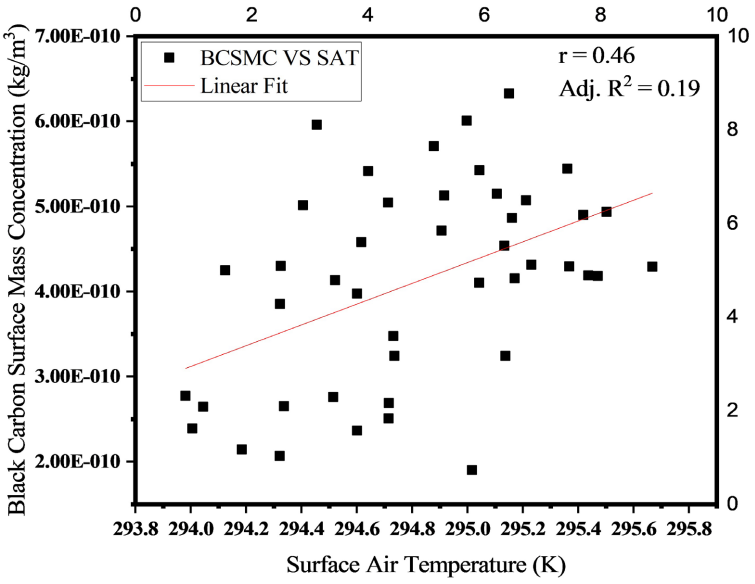

(d)

Figure 8. Seasonal correlation between BC Surface Mass Concentration and Surface Air Temperature averages using (a) DJF, (b) MAM, (c) JJAS and (d) SON seasons over EA during 1980-2023.

Black carbon has a unique ability to absorb sunlight and heat up the atmosphere. When black carbon particles are suspended in the atmosphere, they absorb solar radiation and warm the surrounding air. This leads to an increase in surface air temperature, especially in urban areas and industrial regions where black carbon emissions are high. The warming effect of black carbon can have serious implications for human health, agriculture, and the environment.

In addition to its direct impact on surface air temperature, black carbon can also interact with clouds and alter their properties. Black carbon particles can

serve as cloud condensation nuclei and enhance cloud formation, leading to changes in cloud albedo and precipitation patterns. These interactions between black carbon and clouds can further influence surface air temperature and regional climate dynamics.

During the December-January-February dry season, the study has shown a weak negative correlation of (−0.27) with adjusted R^2 of (0.06) which indicates that only 6% of BC surface mass concentration can be attributed to surface air temperature. This suggests that other meteorological and emission factors play a bigger role than temperature in this time. For instance, reduced DJF precipitation limits wet deposition of aerosols, allowing BC to be reserved in the lower atmosphere. Additionally, stable atmospheric conditions and smaller boundary layer heights are capable of keeping pollutants close to the surface. More aggressive biomass burning for land clearing and heating, especially in rural areas, increases higher BC emissions further. Relative humidity and wind regimes also influence BC distribution by controlling aerosol hygroscopic growth as well as transport dynamics.

4. Summary and Conclusions

Based on a comprehensive analysis of long-term black carbon (BC) surface mass concentration data retrieved from the MERRA-2 reanalysis model for the period 1980-2023, this study has provided in-depth insights into the monthly and seasonal spatial distribution patterns of BC over East Africa, along with its relationship to key meteorological parameters. The main conclusions drawn from the results are summarized as follows:

1) The spatial trends revealed distinct zones characterized by low ($<5 \times 10^{-12}$ kg/m^3), moderate (5×10^{-12} to 8×10^{-12} kg/m^3), and high ($>8 \times 10^{-12}$ kg/m^3) concentrations of BC, with the highest positive trends observed in Western Uganda and northwestern parts of Kenya and Tanzania, particularly during January and February. These trends are primarily attributed to intensified anthropogenic emissions from biomass burning, industrial and vehicular sources, as well as long-range transport of BC aerosols from Asia and the Middle East via easterly winds, and natural emissions from wildfires in West Africa and desert dust from the Sahara transported by westerlies. Air masses carrying BC at lower altitudes (<1500 m) are also thought to enhance regional aerosol loading due to longer residence times and shorter travel distances.

2) Seasonal correlation analyses between BC surface mass concentration and meteorological parameters yielded several notable patterns. Surface wind speed exhibited a consistent and significant inverse relationship with BC levels across all seasons, with stronger negative correlations recorded during June-July-August ($r = -0.50$, $R^2 = 0.24$) and March-April-May ($r = -0.58$, $R^2 = 0.30$). This suggests that increased wind speed enhances dispersion, thereby reducing BC concentrations.

3) Total surface precipitation, on the other hand, showed weak correlations during dry seasons (DJF and JJA), with Pearson's r values of 0.32 and 0.055 and

low adjusted R^2 values of 0.08 and −0.02, indicating that precipitation has limited explanatory power in those periods. However, moderate positive correlations were observed in wet seasons (MAM and SON), with Pearson's r values of 0.37 and 0.41, and adjusted R^2 values of 0.11 and 0.15 suggesting that these observed positive correlations can be attributed to the localized and intermittent nature of rainfall, concurrent increases in anthropogenic emissions, and meteorological conditions that allow pollutant accumulation and regional transport despite ongoing precipitation.

4) Surface specific humidity also demonstrated seasonal variability in its relationship with BC. During dry seasons, correlations were weak ($r \approx 0.34$, $R^2 < 0.10$), whereas wet seasons showed stronger positive correlations, particularly in SON ($r = 0.47$, $R^2 = 0.20$), indicating that specific humidity contributes more significantly to BC concentration variability during periods of higher atmospheric moisture.

5) Surface air temperature showed a weak negative correlation during DJF ($r = -0.28$, $R^2 = 0.06$) and a moderate to strong positive correlation during SON ($r = 0.46$, $R^2 = 0.19$) and JJA ($r = 0.55$, $R^2 = 0.29$), suggesting that temperature-driven atmospheric dynamics may influence aerosol generation and dispersion differently across seasons.

The spatial and seasonal trends of the elevated BC concentrations over East Africa suggest the need for intervention strategies focused on mitigating certain emissions, especially over regions characterized by widespread biomass burning and expanding urban-industrial activities. The key influence of meteorological conditions on BC variability equally emphasizes the necessity for incorporating meteorological forecasting into regional air quality monitoring and management systems. Policymakers can pursue the implementation of early-warning systems and localized mitigation measures that account for seasonally varying pollutant behaviour, especially for periods of increased risk like the dry season and wet transition months. Moreover, with concerted regional action are required to address transboundary pollution from long-range transport. Future scientific research must include high-resolution ground-based measurements to support reanalysis datasets, chemical characterization of the sources of BC to improve discrimination between local and imported emissions, and climate-health impact studies to estimate the more substantial societal costs of BC pollution. These efforts will strengthen the evidence base for successful and contextually relevant air quality policy in East Africa.

Acknowledgements

My deepest appreciation to my supervisors, Prof. John W. Makokha and Dr. Tom Ekisa, for their unwavering support throughout the period of my studies.

Secondly, I acknowledge the National Aeronautics and Space Administration (NASA), specifically the Level-1 and Atmosphere Archive and Distribution System (LAADS) and the Giovanni online data system, for providing and processing the Modern-Era Retrospective Analysis for Research and Applications (MERRA-

2) data used in this study.

Conflicts of Interest

The authors have no conflict of interest whatsoever.

References

[1] Bond, T.C., Doherty, S.J., Fahey, D.W., Forster, P.M., Berntsen, T., DeAngelo, B.J., *et al.* (2013) Bounding the Role of Black Carbon in the Climate System: A Scientific Assessment. *Journal of Geophysical Research*: *Atmospheres*, **118**, 5380-5552. https://doi.org/10.1002/jgrd.50171

[2] Ramanathan, V. and Carmichael, G. (2008) Global and Regional Climate Changes Due to Black Carbon. *Nature Geoscience*, **1**, 221-227. https://doi.org/10.1038/ngeo156

[3] Samset, B.H. (2022) Aerosol Absorption Has an Underappreciated Role in Historical Precipitation Change. *Communications Earth & Environment*, **3**, Article No. 242. https://doi.org/10.1038/s43247-022-00576-6

[4] Williams, M.A., Hemanth Kumar, A., Jayachandran, V., Thakur, M.K. and Kumar, T.V.L. (2024) Effect of Wet Scavenging on Black Carbon Aerosols over a Coastal Urban Site in India. *Air Quality*, *Atmosphere & Health*, **18**, 15-28. https://doi.org/10.1007/s11869-024-01626-y

[5] United Nations Environment Programme. Division of Early Warning, & Assessment (2011) UNEP Year Book 2011: Emerging Issues in Our Global Environment. UNEP/Earthprint.

[6] Buchard, V., Randles, C.A., da Silva, A.M., Darmenov, A., Colarco, P.R., Govindaraju, R., *et al.* (2017) The MERRA-2 Aerosol Reanalysis, 1980 Onward. Part II: Evaluation and Case Studies. *Journal of Climate*, **30**, 6851-6872. https://doi.org/10.1175/jcli-d-16-0613.1

[7] Gelaro, R., McCarty, W., Suárez, M.J., Todling, R., Molod, A., Takacs, L., *et al.* (2017) The Modern-Era Retrospective Analysis for Research and Applications, Version 2 (MERRA-2). *Journal of Climate*, **30**, 5419-5454. https://doi.org/10.1175/jcli-d-16-0758.1

[8] Boiyo, R., Kumar, K.R. and Zhao, T. (2018) Spatial Variations and Trends in AOD Climatology over East Africa during 2002-2016: A Comparative Study Using Three Satellite Data Sets. *International Journal of Climatology*, **38**, e1221-e1240. https://doi.org/10.1002/joc.5446

[9] Pereira, A.G.C., Palácios, R., Santos, P.C.R., Pereira, R.V.S., Cirino, G. and Imbiriba, B. (2024) Relationship between El Niño-Southern Oscillation and Atmospheric Aerosols in the Legal Amazon. *Climate*, **12**, Article No. 13. https://doi.org/10.3390/cli12020013

[10] Nicholson, S.E. (2017) Climate and Climatic Variability of Rainfall over Eastern Africa. *Reviews of Geophysics*, **55**, 590-635. https://doi.org/10.1002/2016rg000544

[11] Camberlin, P. (2018) Climate of Eastern Africa. Oxford Research Encyclopedia of Climate Science.

[12] Wang, H., Kumar, A., Murtugudde, R., Narapusetty, B. and Seip, K.L. (2019) Covariations between the Indian Ocean Dipole and ENSO: A Modeling Study. *Climate Dynamics*, **53**, 5743-5761. https://doi.org/10.1007/s00382-019-04895-x

[13] Randles, C.A., Da Silva, A.M., Buchard, V., Colarco, P.R., Darmenov, A., Go-

vindaraju, R. and Flynn, C.J. (2017) The MERRA-2 Aerosol Reanalysis, 1980 on-Ward. Part I: System.

[14] Khan, R., Kumar, K.R., Zhao, T., Ullah, W. and de Leeuw, G. (2021) Interdecadal Changes in Aerosol Optical Depth over Pakistan Based on the MERRA-2 Reanalysis Data during 1980-2018. *Remote Sensing*, **13**, Article No. 822. https://doi.org/10.3390/rs13040822

[15] Khamala, G.W., Makokha, J.W., Boiyo, R. and Kumar, K.R. (2022) Long-Term Climatology and Spatial Trends of Absorption, Scattering, and Total Aerosol Optical Depths over East Africa during 2001-2019. *Environmental Science and Pollution Research*, **29**, 61283-61297. https://doi.org/10.1007/s11356-022-20022-6

[16] Chin, M., Ginoux, P., Kinne, S., Torres, O., Holben, B.N., Duncan, B.N., *et al.* (2002) Tropospheric Aerosol Optical Thickness from the GOCART Model and Comparisons with Satellite and Sun Photometer Measurements. *Journal of the Atmospheric Sciences*, **59**, 461-483. https://doi.org/10.1175/1520-0469(2002)059<0461:taotft>2.0.co;2

[17] Colarco, P., da Silva, A., Chin, M. and Diehl, T. (2010) Online Simulations of Global Aerosol Distributions in the NASA GEOS-4 Model and Comparisons to Satellite and Ground-Based Aerosol Optical Depth. *Journal of Geophysical Research*: *Atmospheres*, **115**, D14207. https://doi.org/10.1029/2009jd012820

[18] Prospero, J.M., Barkley, A.E., Gaston, C.J., Gatineau, A., Campos y Sansano, A. and Panechou, K. (2020) Characterizing and Quantifying African Dust Transport and Deposition to South America: Implications for the Phosphorus Budget in the Amazon Basin. *Global Biogeochemical Cycles*, **34**, e2020GB006536. https://doi.org/10.1029/2020gb006536

[19] Weatherhead, E.C., Reinsel, G.C., Tiao, G.C., Meng, X., Choi, D., Cheang, W., *et al.* (1998) Factors Affecting the Detection of Trends: Statistical Considerations and Applications to Environmental Data. *Journal of Geophysical Research*: *Atmospheres*, **103**, 17149-17161. https://doi.org/10.1029/98jd00995

[20] Makokha, S.N., Makokha, J.W. and Kelonye, F.B. (2022) Long-Term Assessment of the Spatial Temporal Trends in Selected Cloud Physical Properties over the Three Distinct Sites in Kenya. *Open Access Library Journal*, **9**, 1-18. https://doi.org/10.4236/oalib.1109582

[21] Bi, A., Huang, S. and Sun, X. (2023) Risk Assessment of Oil and Gas Pipeline Based on Vague Set-Weighted Set Pair Analysis Method. *Mathematics*, **11**, Article No. 349. https://doi.org/10.3390/math11020349

[22] Kim, S., Park, H., Jung, H., Lee, J. and Lim, K. (2021) Estimation of Health-Related Physical Fitness Using Multiple Linear Regression in Korean Adults: National Fitness Award 2015-2019. *Frontiers in Physiology*, **12**, Article ID: 668055. https://doi.org/10.3389/fphys.2021.668055

[23] Wang, D., Li, R., Wang, J., Jiang, Q., Gao, C., Yang, J., *et al.* (2020) Correlation Analysis between Disease Severity and Clinical and Biochemical Characteristics of 143 Cases of COVID-19 in Wuhan, China: A Descriptive Study. *BMC Infectious Diseases*, **20**, Article No. 519. https://doi.org/10.1186/s12879-020-05242-w

[24] Jones, T.C., Biele, G., Mühlemann, B., Veith, T., Schneider, J., Beheim-Schwarzbach, J., *et al.* (2021) Estimating Infectiousness Throughout SARS-CoV-2 Infection Course. *Science*, **373**, eabi5273. https://doi.org/10.1126/science.abi5273

[25] Ngo, N.S., Gatari, M., Yan, B., Chillrud, S.N., Bouhamam, K. and Kinney, P.L. (2015) Occupational Exposure to Roadway Emissions and inside Informal Settlements in Sub-Saharan Africa: A Pilot Study in Nairobi, Kenya. *Atmospheric Environment*,

111, 179-184. https://doi.org/10.1016/j.atmosenv.2015.04.008

[26] Mabasi, T. (2009) Assessing the Impacts, Vulnerability, Mitigation, and Adaptation to Climate Change in Kampala City. *World Bank Fifth Urban Research Symposium*, Marseille, June 2009, 28-30.

[27] Ngaina, J.N., Mutai, B.K., Ininda, J.M. and Muthama, J.N. (2014) Monitoring Spatial-Temporal Variability of Aerosol over Kenya. *Ethiopian Journal of Environmental Studies and Management*, **7**, 244-252. https://doi.org/10.4314/ejesm.v7i3.3

[28] Yang, S., Xu, B., Cao, J., Zender, C.S. and Wang, M. (2015) Climate Effect of Black Carbon Aerosol in a Tibetan Plateau Glacier. *Atmospheric Environment*, **111**, 71-78. https://doi.org/10.1016/j.atmosenv.2015.03.016

[29] Boiyo, R., Kumar, K.R. and Zhao, T. (2017) Statistical Intercomparison and Validation of Multisensory Aerosol Optical Depth Retrievals over Three AERONET Sites in Kenya, East Africa. *Atmospheric Research*, **197**, 277-288. https://doi.org/10.1016/j.atmosres.2017.07.012

[30] Ogwang, B.A., Chen, H. and Xing, L.I. (2016) The Effect of Topography on East African Rainfall Based on Regional Climate Model. *Mausam*, **67**, 431-440. https://doi.org/10.54302/mausam.v67i2.1348

[31] Gatebe, C.K., Tyson, P.D., Annegarn, H.J., Helas, G., Kinyua, A.M. and Piketh, S.J. (2001) Characterization and Transport of Aerosols over Equatorial Eastern Africa. *Global Biogeochemical Cycles*, **15**, 663-672. https://doi.org/10.1029/2000gb001340

[32] Makokha, J.W. and Angeyo, H.K. (2013) Investigation of Radiative Characteristics of the Kenyan Atmosphere Due to Aerosols Using Sun Spectrophotometry Measurements and the COART Model. *Aerosol and Air Quality Research*, **13**, 201-208. https://doi.org/10.4209/aaqr.2012.06.0146

[33] de Graaf, M., Tilstra, L.G., Aben, I. and Stammes, P. (2010) Satellite Observations of the Seasonal Cycles of Absorbing Aerosols in Africa Related to the Monsoon Rainfall, 1995-2008. *Atmospheric Environment*, **44**, 1274-1283. https://doi.org/10.1016/j.atmosenv.2009.12.038

[34] Makokha, J.W., Odhiambo, J.O. and Godfrey, J.S. (2017) Trend Analysis of Aerosol Optical Depth and Ångström Exponent Anomaly over East Africa. *Atmospheric and Climate Sciences*, **7**, 588-603. https://doi.org/10.4236/acs.2017.74043

[35] Prijith, S.S., Lima, C.B., Ramana, M.V. and Sai, M.V.R.S. (2021) Intra-Seasonal Contrasting Trends in Clouds Due to Warming Induced Circulation Changes. *Scientific Reports*, **11**, Article No. 16985. https://doi.org/10.1038/s41598-021-96246-2

[36] Khamala, G.W., Makokha, J.W. and Boiyo, R. (2024) The Spatiotemporal and Dependency Analysis of Selected Meteorological Parameters and Normalized Difference Vegetation Index with Aerosol Optical Depth over East Africa. *Heliyon*, **10**, e39961. https://doi.org/10.1016/j.heliyon.2024.e39961

[37] Huang, H., Thomas, G.E. and Grainger, R.G. (2010) Relationship between Wind Speed and Aerosol Optical Depth over Remote Ocean. *Atmospheric Chemistry and Physics*, **10**, 5943-5950. https://doi.org/10.5194/acp-10-5943-2010

[38] Abdullrahman, M. (2022) Possible Association between Space Weather Variables, and the World's COVID-19 Cases. *Journal of Biosciences and Medicines*, **10**, 64-76. https://doi.org/10.4236/jbm.2022.105006

[39] Chakraborty, S., Fu, R., Rosenfeld, D. and Massie, S.T. (2018) The Influence of Aerosols and Meteorological Conditions on the Total Rain Volume of the Mesoscale Convective Systems over Tropical Continents. *Geophysical Research Letters*, **45**, 13-099. https://doi.org/10.1029/2018gl080371

[40] Jiang, Y., Luo, Y. and Zhao, Z. (2013) Maximum Wind Speed Changes over China. *Acta Meteorologica Sinica*, **27**, 63-74. https://doi.org/10.1007/s13351-013-0107-x

[41] Kim, J.J., Hann, T. and Lee, S.J. (2019) Effect of Flow and Humidity on Indoor Deposition of Particulate Matter. *Environmental Pollution*, **255**, Article ID: 113263. https://doi.org/10.1016/j.envpol.2019.113263

[42] Sisterson, D.L., Johnson, S.A. and Kumar, R. (1985) The Influence of Humidity on Fine-Particle Aerosol Dynamics and Precipitation Scavenging. *Aerosol Science and Technology*, **4**, 287-300. https://doi.org/10.1080/02786828508959056

[43] Liu, D., Allan, J., Whitehead, J., Young, D., Flynn, M., Coe, H., *et al.* (2013) Ambient Black Carbon Particle Hygroscopic Properties Controlled by Mixing State and Composition. *Atmospheric Chemistry and Physics*, **13**, 2015-2029. https://doi.org/10.5194/acp-13-2015-2013

[44] Kumar, R.P., J., B., Samuel, C. and Gautam, S. (2022) A Bibliometric and Scientometric: Analysis towards Global Pattern and Trends Related to Aerosol and Precipitation Studies from 2002 to 2022. *Air Quality*, *Atmosphere & Health*, **16**, 613-628. https://doi.org/10.1007/s11869-022-01290-0

[45] Gupta, P., Singh, S.P., Jangid, A. and Kumar, R. (2017) Characterization of Black Carbon in the Ambient Air of Agra, India: Seasonal Variation and Meteorological Influence. *Advances in Atmospheric Sciences*, **34**, 1082-1094. https://doi.org/10.1007/s00376-017-6234-z

[46] Hill, P.G., Stein, T.H.M. and Cafaro, C. (2023) Convective Systems and Rainfall in East Africa. *Quarterly Journal of the Royal Meteorological Society*, **149**, 2943-2961. https://doi.org/10.1002/qj.4540

[47] Jacobson, M.Z. (2001) Strong Radiative Heating Due to the Mixing State of Black Carbon in Atmospheric Aerosols. *Nature*, **409**, 695-697. https://doi.org/10.1038/35055518

[48] Morton, D.C., DeFries, R.S., Shimabukuro, Y.E., Anderson, L.O., Del Bon Espírito-Santo, F., Hansen, M., *et al.* (2005) Rapid Assessment of Annual Deforestation in the Brazilian Amazon Using MODIS Data. *Earth Interactions*, **9**, 1-22. https://doi.org/10.1175/ei139.1